Int. J. Multiphase Flow Vol. 14, No. 5, pp. 533–546, 1988
Printed in Great Britain.

0301-9322/88 $3.00 + 0.00

HINDERED SETTLING AND HYDRODYNAMIC DISPERSION IN QUIESCENT SEDIMENTING SUSPENSIONS

J. M. HAM and G. M. HOMSY
Department of Chemical Engineering, Stanford University, Stanford, CA 94305, U.S.A.

(*Received* 2 *December* 1987; *in revised form* 5 *May* 1988)

Abstract—The motion of an individual sphere settling in the midst of a suspension of like spheres has been examined experimentally for suspensions with volume concentrations, ϕ, of 2.5–10%, under creeping flow conditions and in the absence of Brownian motion. In the experiments, silvered glass spheres were tracked in optically transparent suspensions of glass beads. Arrival times measured at a series of horizontal planes were converted into average settling speeds. These average speeds yield the hindered settling speed as a function of concentration. The hindered settling speed, normalized by the isolated sphere settling speed, exhibits a $1 - 4\phi + 8\phi^2$ dependence for the range of concentrations investigated. The settling speed fluctuations are quite large, ranging up to 46% of the average, and have long-time (large settling distance) behavior characteristic of a Fickian diffusion process. Dispersion coefficients have therefore been determined from the asymptotic dependence upon settling distance of the variance in settling speed. These coefficients scale with the product of the hindered settling speed and the sphere radius. The dimensionless dispersion coefficients, all $O(1)$, increase with concentration for $\phi < 5\%$, then slightly decrease at higher concentrations. Verification of the scaling through the use of two particle sizes, care taken to mix the suspensions to random, uniform initial conditions, and the robustness of the statistics over many realizations preclude the possibility of this phenomenon being an experimental artifact and support the hypothesis that hydrodynamic dispersion of suspended particles will result from viscous interactions between the particles.

Key Words: sedimentation, hydrodynamic dispersion

1. INTRODUCTION

The velocity of a particle in the midst of a flowing suspension of particles can be divided into two parts: a mean velocity, $\langle \mathbf{V} \rangle$; and a fluctuation, $\mathbf{V}'$. In quiescent sedimentation, i.e. the settling out under gravity of particles suspended in a quiescent fluid, the mean velocity determines the sedimentation rate and the fluctuations influence, among other things, the spread of the interface between the sedimenting suspension and the growing clear fluid layer above. In fluidization, the mean velocity is the fluidizing velocity relative to a translating frame, and the velocity fluctuations contribute to the response of the fluid bed to perturbations in the local particle concentration. Understanding both parts of the particle velocity is therefore quite important in understanding the macroscopic behavior of systems of suspended particles.

In quiescent sedimentation under creeping flow conditions, the mean velocity will be in the direction of gravity and have a magnitude, $\langle V \rangle$, proportional to the Stokes settling speed V_0. The proportionality factor, f, known as the hindered settling function, is dependent upon the volume concentration of particles in the suspension, ϕ. The nature of the dependence is dictated by the suspension microstructure, i.e. the details of the relative positions of the particles [summarized by Saffman (1973)]. If the particles are arranged in a regular lattice, then $1 - f(\phi)$ is proportional to $\phi^{1/3}$, as $\phi \to 0$. If the particles are arranged in a random fashion, with their relative positions fixed, then $1 - f(\phi)$ is proportional to $\phi^{1/2}$, as $\phi \to 0$. If the particles are arranged in a random fashion, with their relative positions free to change in order to maintain a given net force, than $1 - f(\phi)$ is proportional to ϕ, as $\phi \to 0$.

The case of a random, free suspension is the one most likely to occur in processes of practical interest, yet is in some ways the most difficult to handle theoretically. Because the particles are free to adjust their relative positions, a complete analysis of random, free suspensions must account for any adjustments of the microstructure which may occur due to the flow field in the suspension. This complication adds to the already imposing problem of considering interactions among many particles, interactions with effects which diminish quite slowly with distance. The long range of

interactions can lead to divergent integrals when summing the contributions to the velocity at a point in the suspension from an indefinitely large number of particles distributed randomly throughout the suspension. The problem of the divergent integrals was overcome by Batchelor (1972), using a renormalization technique to calculate the first, or $O(\phi)$, correction to the mean settling speed. In order to make an explicit calculation, Batchelor considered a "well-stirred" suspension of identical spheres, a suspension in which all particle positions are equally likely, and found $\langle V\rangle/V_0 = 1 - 6.55\phi$, as $\phi \to 0$. (Here, and in the remainder of this paper, "$\langle\ \rangle$" denotes an ensemble average.) Batchelor also showed, in his section 7, the $O(\phi)$ coefficient to be sensitive to the details of the random configuration of the suspension, e.g. a configuration favoring close pairs will have a lower coefficient. These considerations have been clarified and amplified by Hinch (1977), who, among other things, gives a compact expression for the $O(\phi)$ coefficient which involves the radial-distribution function characterizing the microstructure.

Analysis of the mean settling speed leaves unresolved the problem of microstructural evolution in suspensions. Such changes in the relative positions of particles are likely because each particle in a random suspension sees a slightly different local environment and is therefore expected to have a velocity which is, in general, different from that of any neighboring particle. The variations in particle velocities will lead to an adjustment of the particle distribution. Evidence that such evolution may be significant can be drawn from an analysis due to Caflisch & Luke (1985) which extended the analysis of Batchelor (1972) to the variance in the settling speed. Caflisch & Luke found the variance to diverge as the number of particles in the suspension is allowed to increase without limit. This counterintuitive result may be an indication that the "well-stirred" particle distribution cannot be maintained in sedimentation, and that more information about the microstructure is required to understand the behavior of the velocity fluctuations.

The first step in understanding the nature of the velocity fluctuations is understanding the mechanism that leads to the fluctuations. In a random suspension, some particles will be separated from their nearest neighbors by distances which are less than the average interparticle spacing. These close pairs will fall at speeds above the mean, and therefore overtake other, slower-settling particles. The ensuing three- and higher-body interactions will result, even under conditions of creeping flow, in a net displacement of particles. The net displacement will produce a change in the particle distribution and therefore a change in the particle velocities. The process of multibody interactions and configuration changes will continue as sedimentation proceeds. The random positions of the particles and a large number of interactions are expected to cause the details of individual interactions to be lost and an individual particle to execute a random walk through the suspension. Such a random walk process leads naturally to a description of particle migrations as a Fickian process.

Particle migrations resulting from hydrodynamic interactions among particles, which will be termed "hydrodynamic dispersion", will, in general, be anisotropic since the velocity fluctuations parallel to the mean velocity may differ from those perpendicular to the mean. Hydrodynamic dispersion must therefore be characterized by a dispersion tensor, in contrast to the scalar coefficient which characterizes isotropic diffusion arising from Brownian motion. For the remainder of this paper, however, only one component of the dispersion tensor, that parallel to gravity, will be considered.

Once an analogy to Fickian diffusion is made, the associated dispersion coefficient, D, can be defined in terms of the long-time behavior of the distribution of particle positions, i.e.

$$D = \lim_{t\to\infty} \frac{\delta^2}{2t}, \qquad [1]$$

where δ^2 is the variance from some mean particle position at time t. In a sedimenting suspension δ^2 can be replaced with $\sigma_v^2 t^2$ where σ_v^2 is the variance from the mean particle speed measured over a time t. The substitution yields a more accessible form for D, i.e.

$$D = \lim_{t\to\infty} \frac{\sigma_v^2 t}{2}. \qquad [2]$$

The hydrodynamic dispersion coefficient will scale with the appropriate length scale, l_c, and the scale t_c, for a given system, so that $D \sim l_c^2/t_c$. The characteristic length in turn will scale with the

distance travelled between interactions, which is related to the interparticle spacing, which is proportional to the particle radius, a. The characteristic time will be the time required to travel that distance, which in sedimentation is proportional to $a/\langle V \rangle$. D therefore scales with $\langle V \rangle a$. This simple scaling results directly from dimensional considerations, once the assumptions of creeping flow of non-Brownian particles are made. The dimensionless coefficient, $\hat{D}$, will, in general, have a dependence upon ϕ and the details of the microstructure. The microstructural dependence arises from the fact that the time between interactions is related to the difference between the velocities of the faster- and slower-setting particles, and the difference will be influenced by the relative positions of the particles. The influence of ϕ comes about from the change in interparticle spacing with concentration of particles.

Previous investigations of hydrodynamic dispersion of suspended particles have been made for both sheared and sedimenting suspensions. Dispersion coefficients in sheared, monodisperse suspensions of spheres have been determined experimentally by Eckstein *et al.* (1977) and Leighton & Acrivos (1987). Leighton & Acrivos showed the coefficient in shear flow to scale with the product of the shear rate and a^2, and to be proportional to ϕ^2 as $\phi \to 0$. Dispersion coefficients in quiescent sedimentation have been examined experimentally by Davis & Hassen (1988). A summary of the portion of their study related to hydrodynamic dispersion is given below.

The experiments by Davis & Hassen investigated the spreading of the interface between a sedimenting, slightly-polydisperse suspension of spheres and the growing clarified fluid layer above. Davis & Hassen observed that the interface spread was greater than that predicted to arise from polydispersity and found the additional spreading could be attributed to dispersion. Dispersion coefficients were then inferred from initial spreading rates. The dispersion coefficients were nondimensionalized with the product of a median settling speed and particle radius, but the scatter in the dimensionless coefficients precludes any definitive conclusion as to the proper scaling. Their measurements, made at an interface, where a gradient in volume concentration of spheres was present, result in coefficients which will, in general, differ from coefficients measured within a region of uniform concentration. The experiments to be described herein measured directly the velocity fluctuations of an individual particle within the bulk of a suspension.

Our objective was to characterize the nature of the movements of an individual particle settling in the midst of a suspension of like particles. The conceptually simple experiment designed to accomplish our objective was one in which a single sphere, marked with a thin coating of silver, was visually tracked in a suspension of unmarked glass spheres, made optically transparent by matching the index of refraction of the suspending fluid to that of the glass spheres. The marked sphere was timed as it settled past a series of horizontal planes in the suspension. The arrival times provided information on the settling speed necessary to find the hindered settling function and to examine the validity of describing hydrodynamic dispersion of suspended particles as a Fickian process.

Presentation of our work begins with a description of the experimental system and procedure in section 2. Section 3 contains an overview of the method applied to analyze the experimental data. The results of the data. The results of the data analysis are discussed in section 4 and conclusions are summarized in section 5.

2. EXPERIMENTAL SYSTEM AND PROCEDURE

The combinations of fluid and particles used in the experiments were chosen to meet several criteria. First, the fluid and particles were to have the same index of refraction so that suspensions would be optically transparent, except for small bubbles and imperfections in the particles. An optically transparent suspension would allow observation of the test particle anywhere in the suspension. Second, the particles were to be large enough for simple visual tracking of any marked particle. Third, the fluid was to be viscous enough to maintain creeping flow conditions. Meeting the second and third criteria automatically satisfied the requirement that the effects of Brownian motion be unimportant. The fluid selected was Santicizer 278 produced by Monsanto. Santicizer 278 is a benzyl phthalate plasticizer with index of refraction 1.51, density $\rho = 1080\ \mathrm{kg/m^3}$ and kinematic viscosity $\nu = 8.45 \times 10^{-4}\ \mathrm{m^2/s}$ at 24°C. The particles chosen were glass beads with index of refraction 1.51 and density $\rho_s = 2420\ \mathrm{kg/m^3}$. Two sizes of glass beads were used, one batch with

a diameter range of 595–707 μm and one of 420–500 μm. These combinations kept the particle Reynolds number, $2aV_0/\nu$, $<10^{-4}$ and the Brownian Péclet number, $6\pi\rho\nu a^2 V_0/kT$, $>10^{11}$ for all experiments.

The particles, nominally between two adjacent mesh sizes when shipped from the manufacturer, were carefully rescreened to eliminate particles outside the desired size ranges. The rescreening consisted of two steps: vigorously shaking the particles on the undersize screen until no more particles would pass through then repeatedly passing the batch through the oversize screen, with only gentle shaking, until the particles passed through the screen without leaving any behind. Nonspherical and opaque particles were removed from the remaining particles by careful inspection. The density of the screened particles was checked by determining the weight of glass beads required to displace a known volume of liquid.

Representative test particles were selected from each batch of screened glass beads. Each test particle was required to be nearly spherical and to have the same settling speed as any other representative particle in the suspension, i.e. to be "hydrodynamically" identical to the suspended particles. These test particles were marked for visual tracking with the suspensions. Silvering was chosen as the method of marking particles because the uniformly smooth, thin coating of silver had inconsequential effects on settling characteristics yet made the marked particle easily visible. Several potential test spheres were silvered using the Brashear chemical silvering process (Strong 1938). The silvered spheres were characterized by isolated sphere settling experiments. The test sphere chosen for a given size range was one with a settling speed, V_0, which was repeatable to within 1.0% and close to that expected to be representative of that set of particles.

All experiments were performed in glass columns of circular cross-section maintained at constant temperature by a temperature-controlled water bath. Two different glass columns were used: one of 6.0 cm dia for the larger particles; and one of 4.7 cm dia for the smaller particles. Each column had a height of 30 cm. The column diameters were chosen to be large enough to avoid serious wall effects, but small enough to alleviate bulk convection current problems described later in this section. The column height was chosen to allow the suspension enough distance for sedimentation to reach long-time behavior, i.e. for the variance in sedimentation speed to reach some asymptotic dependence upon settling distance. During the experiments the column in use was held in fixed position, with the column walls vertical, by tabs attached to the bottom of the water bath.

Suspensions were made by filling the experimental column with a known volume of Santicizer 278 then adding enough particles to reach the desired volume concentration. The concentration of the suspension was checked between every few runs by measuring the weights of the filled column and the height of the fluid in the column. This information, coupled with a knowledge of ρ, ρ_s, the empty column weight and the cross-sectional area of the column, allowed a simple determination of the volume fraction of particles. The concentration from run to run varied by no more than 0.1%

Suspensions were brought to initial conditions with a two-stage mixing process. The first stage distributed the particles nearly uniformly throughout the suspending fluid. The second stage smoothed out small regions in which the particle concentration differed significantly from the bulk concentration. The regions of inhomogeneities were visually identified by coherent convection currents which did not show signs of being damped by viscous forces. Preliminary mixing was carried out with an auger driven by a variable-speed drill motor. The auger, coated with epoxy to prevent oxidation by the fluid, had a diameter of approx. 2.5 cm. Final mixing was accomplished with a thin, glass stirring rod. The stirring rod had a diameter of approx. 3 mm.

The test particle was placed into the suspension through a glass pipette having a long, slender tip of diameter only slightly larger than the particles. The pipette slid into a bracket placed against guides on top of the water bath above the experimental column. The two-piece launching system was a simple means of forcing the test particle to enter the suspension at the same position at the start of each sedimentation run.

Each sedimentation run consisted of mixing the suspension, launching the test particle and measuring a sequence of arrival times of the test particle at a set of horizontal planes. The procedure for each run was identical. First, the auger was placed in the suspension until thermal equilibrium was reached. Next, preliminary mixing began, continuing 2–3 min beyond the time at which the particles appeared to have a random, uniform distribution throughout the suspension. Upon

completion of the preliminary mixing, the mixer was slowly removed from the column, taking care not to sweep particles into a wake behind the auger. The auger was placed in a beaker during the ensuing run to collect for reuse any residual suspension. Then, final mixing insured attainment of a homogeneous initial state.

After achieving the desired initial conditions, the suspension was allowed to settle for a short time. During this time an interface formed between the suspension and a growing layer of clear fluid at the top of the column. The test particle was introduced into the suspension when this interface reached a predetermined horizontal plane. The position of the plane was such that the test particle entered the suspension approx. 3 cm below the interface and 3 cm above the horizontal plane at which tracking would begin.

A cathetometer was set to view the initial horizontal plane and timing began when the test particle arrived at the plane. The cathetometer was reset to a plane 1 cm below the previous plane, then the arrival time and transverse position at the plane were logged into a small laboratory computer. Figure 1 contains a schematic of the column and the cathetometer. This procedure was repeated until the test sphere had fallen 10 cm. (A total settling distance of 12 cm was used for $\phi = 2.5\%$. This larger distance was deemed necessary, with the larger interparticle spacing, to provide enough time to reach asymptotic behavior.) After the run, the test sphere was retrieved and the mixer was placed back in the column for thermal equilibration. Any fluid and particles recovered in the beaker were poured back into the column to maintain the proper level and concentration.

Additional observations of the interior of the suspension were made as each run progressed. These observations were to check for the bulk convection currents due to imperfections in the mixing. "Imperfections in mixing" are not the expected random variations in the particle distribution, but are variations in the concentration of particles over length scales of the order of the vessel size. Variations in the concentration produced gradients in the effective density of the suspension which drive convection currents. The strength of these convection currents is proportional to L^3, where L is the distance over which the density gradient extends. Since L can be of the order of the vessel size, excursions from the mean speed due to convection currents can dominate the motion of particles during sedimentation. The bulk convection currents, which persist

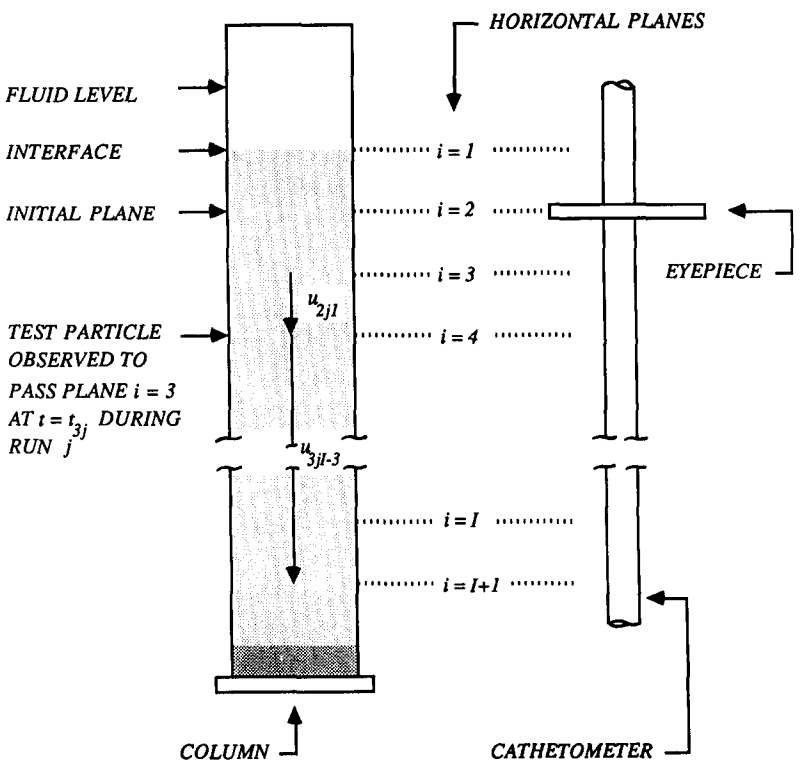

Figure 1. Schematic diagram of a sedimentation column.

throughout the course of sedimentation, produce coherent structures in the midst of the suspension having little effect upon the interface between the suspension and the clear fluid. Only careful observations of the interior of the suspension can reveal existence of these currents. Runs during which coherent structures persisted were stopped and eliminated from the data base. Further statistical tests, described in section 3, were used to eliminate data from runs which, although not visually affected by such currents, may have been influenced by poor mixing.

The position of the interface relative to the test particle was also monitored during the course of each run, as an additional consistency check. The definition of the interface position was somewhat subjective since all observations were visual and interface spread was not quantitatively accounted for. The interface, however, appeared quite sharp for all runs except those at $\phi = 2.5\%$, so the trends in the observed average interface speed and the trends in the average particle settling speed should exhibit the same qualitative behavior.

Enough sedimentation runs were made for a given concentration and particle size to provide a statistically satisfactory data base, the criteria for which will be described in the section 3. The number of runs required to meet these criteria was typically between 20 and 30.

3. DATA ANALYSIS

The main objectives of the experiments were to measure the mean settling speed as a function of ϕ and to determine the long-time behavior of the fluctuations in the settling speed. To meet these ends, the data were analyzed to a two-stage process: first, the statistical significance of the data base was evaluated; second, expected values and confidence intervals for all the quantities of interest were calculated. The details of this analysis are presented in this section.

An average settling speed for each run was calculated from the total settling time and the total settling distance. A cumulative average, U_j, and standard deviation, ΔU_j, of these speeds were maintained as runs, j, were added to the data base for each experimental series. When U_j and ΔU_j reached stationary values the data base was deemed sufficient to produce meaningful statistics. Figures 2a and 2b show typical evolutions of U_j and ΔU_j with the number of runs included in the data set for $\phi = 5.0\%$ and $2a = 470\,\mu$m. [For a complete set of figures see Ham (1988).] The fact that U_j and ΔU_j attained values which did not change appreciably with the size of the data base indicated that additional runs, while improving the confidence intervals for various statistical quantities, would provide little new information about the expected values of those same quantities.

Detailed data reduction began with conversion of arrival times into a sequence of speeds calculated over intervals ranging in size from 1 to 10 cm (12 cm in the 2.5% case) in 1 cm increments. Sample means, V_k, and variances, S_k^2, of the speeds were determined for each interval size. With reference to figure 1, these quantities were calculated as follows:

$$u_{ijk} = \frac{k}{t_{i+k,j} - t_{ij}}, \qquad [3]$$

$$V_k = \frac{\sum_{i=1}^{K} \sum_{j=1}^{J} u_{ijk}}{N} \qquad [4]$$

and

$$S_k^2 = \frac{\sum_{i=1}^{K} \sum_{j=1}^{J} (u_{ijk} - V_k)^2}{N - 1}, \qquad [5]$$

where

t_{ij} = arrival time at horizontal plane i during run j,
i = horizontal plane number $(0, 1, 2, \ldots, I)$,
j = run number,
k = interval size $(1, 2, \ldots, I)$,
J = total number of runs in series,
K = number of intervals of size k in a run, $I + 1 - k$

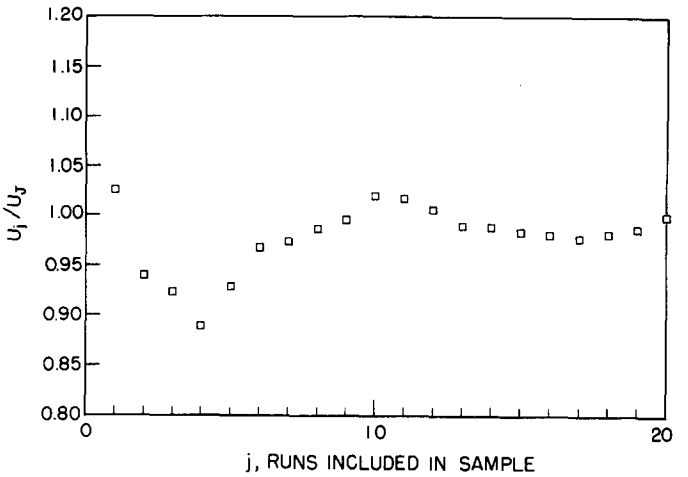

Figure 2a. Evolution of cumulative average sedimentation speed with the number of runs included in the statistical sample, for 470 μm particles at $\phi = 5.0\%$.

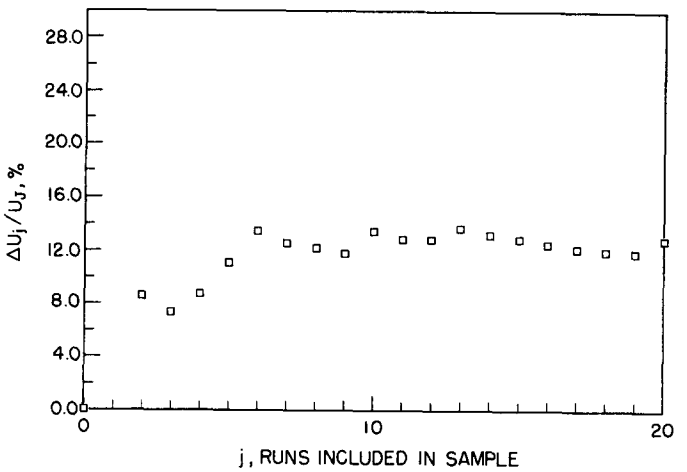

Figure 2b. Evolution of standard deviation from cumulative average sedimentation speed with the number of runs included in the statistical sample, for 470 μm particles at $\phi = 5.0\%$.

and

$$N = K \times J.$$

The hypothesis that an individual particle executes a random walk, described in section 1, requires normal distributions of speeds for interval sizes large enough to exhibit asymptotic behavior. Neither the validity of such a hypothesis nor the interval size requirement for long-time behavior were known *a priori*, so the data were treated under the assumption that speeds for all interval sizes fell in normal distributions. The normal distribution assumption also allowed calculation of confidence intervals for the means and variances of the speeds (Meyer 1970) and gave a good criterion for eliminating outlying data. Any run was an interval speed falling outside the range of $V_k \pm 4 \times (S_k^2)^{1/2}$ was eliminated from the data set. This criterion eliminated only a few runs from each data set.

The random walk hypothesis also predicts that the settling speed of a particle will become uncorrelated with its initial settling speed after some characteristic time τ. If τ is less than the average time required for the particle to travel a certain number of intervals, then the particle can be considered to begin a new realization after traveling that number of individual. We did not know τ, so we performed serial correlations with the 1 cm interval speeds for each run. Correlation coefficients between adjacent intervals within a run rarely exceeded 0.5 and average coefficients for a series of runs were typically around 0.3. We therefore considered interval speeds sufficiently

Table 1. Summary of sample statistics for 470 μm particles at $\phi = 5.0\%$ ($V_0 = 17 \times 10^{-4}$ m/s, $V_I/V_0 = 0.84$, $I = 10$, $J = 20$)

		V_k/V_I			$100 \times S_k^2/V_k^2$		
			90% Confidence limits			90% Confidence limits	
k	$h/2a$	Sample mean	Lower	Upper	Sample mean	Lower	Upper
1	21.3	1.16	1.10	1.21	21.0	16.8	27.5
2	42.6	1.08	1.04	1.13	13.2	10.5	17.3
3	63.8	1.05	1.01	1.09	8.98	7.16	11.7
4	85.1	1.03	0.98	1.06	7.23	5.76	9.45
5	106.4	1.01	0.97	1.05	5.76	4.59	7.53
6	127.7	1.00	0.96	1.04	4.73	3.77	6.18
7	148.9	0.99	0.96	1.03	3.70	2.91	4.93
8	170.2	1.00	0.96	1.04	3.37	2.56	4.73
9	191.5	1.00	0.95	1.04	2.97	2.12	4.51
10	212.8	1.00	0.94	1.06	2.64	1.66	4.96

uncorrelated to allow us to expand our statistical base by considering the test particle to have started a new realization, of correspondingly shorter overall duration, at each horizontal plane i. The expanded data base improved our confidence limits but had little other effect. A complete description of the serial correlations can be found in Ham (1988).

An example of the sample statistics for the series of runs at $\phi = 5.0\%$ and $2a = 470\,\mu$m is presented in table 1. [For a complete set of tables see Ham (1988).] Two important features of the statistics in table 1 should be noted. First V_k becomes constant at larger values of k, therefore V_I is taken as the best estimate of $\langle V \rangle$. The initial dependence of V_k upon k is the result of our measurement technique. We did not measure instantaneous speeds and time-average them over the time required to traverse an interval, but instead measured the total time required to settle through an interval and used distance/time as the average speed. The two types of averages are different, but their ensemble averages approach the same value as the interval size becomes large (Ham 1988). Second, the sample variances, taken to be estimates for σ_v^2, decrease significantly and monotonically with increasing interval size. The means and variances from table 1 and from the sets of statistics for the other series of runs are used in section 4 to yield results on hindered settling and hydrodynamic dispersion.

4. RESULTS AND DISCUSSION

Hindered Settling

Figure 3 presents V_I calculated at fixed postions i, in the column for $\phi = 5.0\%$ and $2a = 470\,\mu$m. That this mean settling speed has no correlation with interval position is evidence for considering sedimentation in the experimentally examined region of the column to be representative of sedimentation in a bulk suspension. In other words, the lack of any significant trend in the mean settling speed as the test particle moved down through the column indicates that no transients due to poor mixing, disturbances from the injection procedure, the spreading of the suspension interface, or the growth of the sediment layer on the bottom of the column were present.

Table 2 and figure 4 present the experimentally determined dependence of $\langle V \rangle / V_0$ upon ϕ. The interface speed, $u(\phi)$, is presented in figure 4 as $(u(\phi)/V_0) \times (V_I/u)_{\phi = 5\%}$ to avoid difficulties with estimating u_0. Two important features of figure 4 should be noted. First, the dimensionless settling speeds for two different particle sizes at $\phi = 5\%$ match within 90% confidence intervals, so we shall consider scaling the hindered settling speed with V_0 to be appropriate, as is generally accepted. Second, the interface speed and the single particle speed diverge at $\phi = 10\%$, raising a question about the validity of the 10% data. The second feature will be examined in more detail.

V_I at $\phi = 10\%$ is suspect because this point does not coincide with the expectation that the slope of $f(\phi)$ becomes less steep outside the dilute concentration region. Following up on the suspicion, two different quadratic least-squares fits were made to the data: one including all the V_I/V_0 and another excluding V_I/V_0 at $\phi = 10\%$. The results of these fits are presented in table 3 and

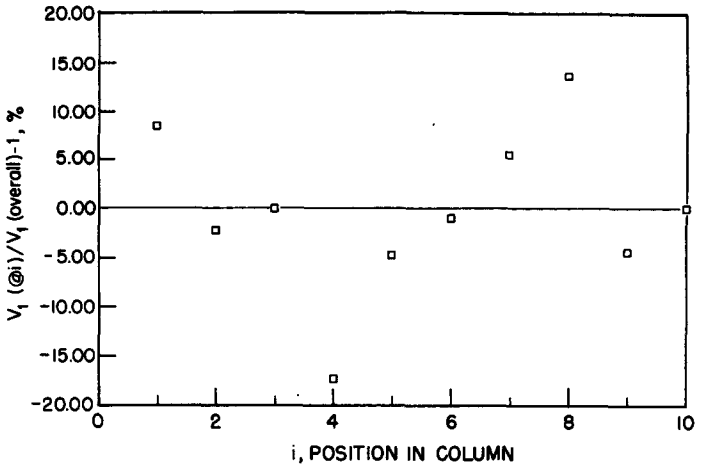

Figure 3. Deviation of V_1 calculated at set positions in the column from V_1 calculated for all 1 cm intervals, for 470 μm particles at $\phi = 5.0\%$.

Table 2. Mean settling speeds and 1 cm interval fluctuations

		V_1/V_0		
ϕ (%)	$2a$ (μm)	Mean	90% Confidence interval (%)	$(S_1^2/V_1^2)^{1/2}$ (%)
2.5	650	0.89	±5	25
5.0	470	0.84	±6	46
	650	0.81	±5	39
8.0	650	0.73	±6	45
10.0	650	0.61	±5	43

Table 3. Hindered settling function least-squares regression results

	CV[a] over indicated region (%)	
Regression curve	$0 < \phi < 8\%$	$0 < \phi < 10\%$
$0.99 - 2.9\phi - 7.1\phi^2$	2.6	2.5
$1.0 - 3.9\phi + 8.2\phi^2$	1.8	4.8

[a]CV = coefficient of variance (Myers 1986).

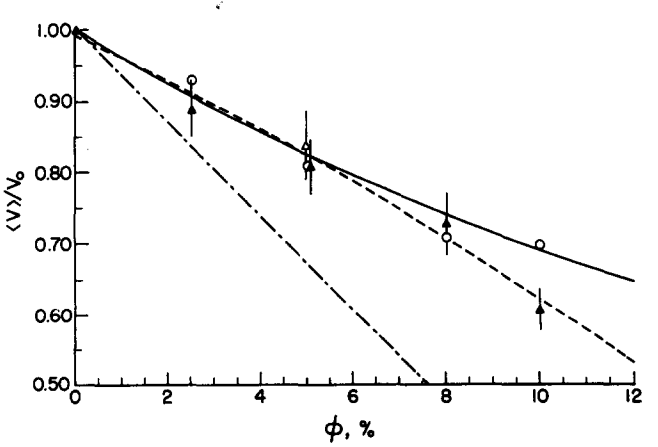

Figure 4. Hindered settling function: ▲, $2a = 650\,\mu$m; △, $2a = 470\,\mu$m; ○, interface data for $2a = 650\,\mu$m; ——, $1 - 3.9\phi + 8.2\phi^2$; – – –, $0.99 - 2.9\phi - 7.1\phi^2$; ———, Batchelor (1972). Error bars on the experimental values represent 90% confidence intervals.

figure 4. The fit with all the data, $f(\phi) = 0.99 - 3.0\phi - 7.1\phi^2$, is unsatisfactory because of the negative coefficient for the ϕ^2 term. The latter fit, $f(\phi) = 1.00 - 3.9\phi + 8.2\phi^2$, is more satisfying for two reasons. First, the curve comes very close to predicting the interface speed at $\phi = 10\%$. The exact relationship between an interface settling speed and the settling speed of an individual particle in the bulk is not entirely clear, but the sharpness of our interfaces for $\phi \geqslant 5\%$ prompted us to use this as a qualitative check. Second, the curve is nearly the same as that from a Richardson–Zaki (1954) correlation, $f(\phi) = (1 - \phi)^n$, with $n = 4$, which would expand to $1 - 4\phi + 6\phi^2 + O(\phi^3)$. Some problem with the mean settling speed at $\phi = 10\%$ therefore seems likely. Unfortunately, no explanation for the problem with the 10% settling speed can be given at this time. The data from that runs series exhibited, in all other respects, the same qualitative behavior as the data from all the other series of runs.

Both estimates of the $O(\phi)$ coefficient are significantly below the value of 6.55 arising from the analysis of Batchelor (1972), in which a "well stirred", monodisperse suspension is assumed. Our suspensions were slightly polydisperse, so a comparison with the work of Batchelor (1982) and Batchelor & Wen (1982) is more applicable. The limit of a nearly-monodisperse suspension of equidensity spheres in Batchelor & Wen is complicated, but in the limit of negligible Brownian motion effects the $O(\phi)$ coefficient is bounded from below by 5.6. Still, our value of 4 is lower. These discrepancies suggest a more complicated microstructure, the nature of which may only be accessible through simulations, such as those described in Durlofsky *et al.* (1987).

Finally, we quote for comparison one other recent set of experimental results on hindered settling—those of Davis & Birdsell (1988). Davis & Birdsell determined the hindered settling function by measuring the settling speed of the interface between a suspension and the clear fluid above. Comparisons of our results with interface measurements, which are readily available in the literature, are made difficult by the fact that the interface spreads during sedimentation (Davis & Hassen 1988). Each layer in a spreading interface has its own distribution of particle sizes and local value of ϕ, thus complicating the relationship between the settling speed of layers in the interface with that of an individual particle somewhere in the bulk of the suspension. Davis & Birdsell, who were very careful in characterizing their suspensions and interfaces, found the settling speed of the horizontal plane in the interface with a local value of ϕ equal to half the bulk value could be described by a Richardson–Zaki correlation with $n = 5$, when that speed was normalized with the Stokes settling speed of a sphere with the median particle diameter. The Davis & Hassen result lies between the Batchelor (1972) or Batchelor & Wen (1982) result and our experimental data.

Hydrodynamic Dispersion

The most striking aspect of the observed variances in settling speed is their magnitude. As the results in table 2 show, the 1 cm interval fluctuations ranged from 25 to 46% of the mean. In addition, the variances in settling speed were observed to depend upon the interval size, with the variance decreasing with increasing interval size. The variance in settling speed decreases linearly with the inverse of the settling distance, or interval size, for the random walk process. This linear dependence on the inverse settling distance arises when the settling time, t, in [2] is replaced with $h/\langle V \rangle$, where h is the settling distance. The relation for the dimensionless dispersion coefficient, $\hat{D} = D/\langle V \rangle a$, then becomes

$$\hat{D} = \lim_{H \to \infty} \sigma^2 H;$$

$$\sigma^2 = \frac{\sigma_v^2}{\langle V \rangle^2}$$

and

$$H = \frac{h}{2a}. \qquad [6]$$

The random walk hypothesis therefore requires that the slope, α, of a log–log plot of σ^2 vs H be -1 in the limit of large H. Figure 5a presents an example of such a log–log plot and the resulting least-squares fit for $\phi = 5.0\%$ and $2a = 470\ \mu$m [see Ham (1988) for a complete set of figures]. The

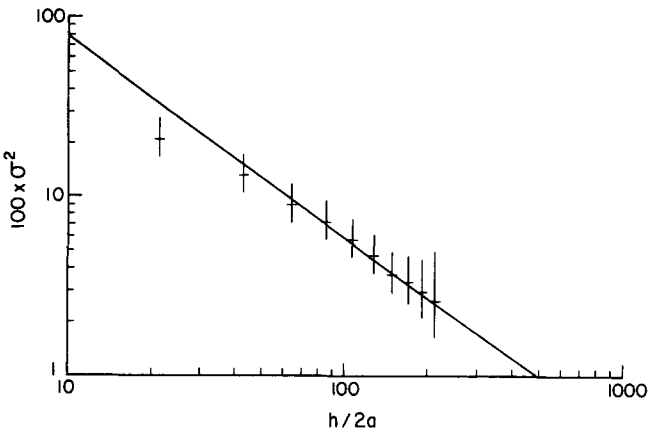

Figure 5a. Asymptotic behavior of σ^2 as $H \to \infty$ for 470 μm particles and $\phi = 5.0\%$. Error bars on the experimental values represent 90% confidence intervals. The best-fit line is from a linear regression including only data for $H > H_\infty$.

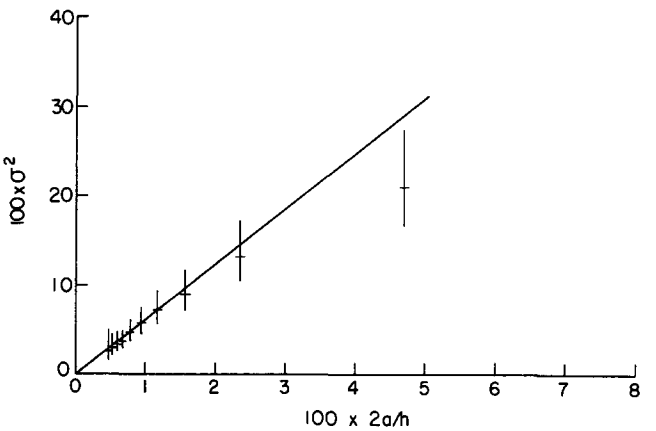

Figure 5b. Asymptotic behavior of σ^2 as $1/H \to 0$ for 470 μm particles and $\phi = 5.0\%$. Error bars on the experimental values represent 90% confidence intervals. The best-fit line is from a linear regression including only data for $1/H < 1/H_\infty$.

fact that $\alpha = -1$, within 90% confidence limits, for each data set, as shown in table 4, provides evidence that the variance behaves as it should for a random walk process, justifying description of particle migrations in sedimentation as a Fickian process.

The distance, H_∞, at which the fluctuations have reached asymptotic behavior determines the data points which should be included in a least-squares regression. This distance is not known *a priori*, and since [6] is only an *asymptotic* relation, H_∞ is a vaguely defined quantity. The nature

Table 4. Random walk verification least-squares regression results: $\sigma^2 = \hat{D} \times H^\alpha$

			α[a]		$\hat{D}$[b]			
					90% Confidence limits			
ϕ (%)	$2a$	H_∞	Mean	90% Confidence interval	Mean	Lower	Upper	CV (%)
2.5	650	77–92	−1.00	±0.05	2.1	1.8	2.4	2.7
5.0	470	64–85	−1.05	±0.05	7.4	6.6	8.4	1.1
	650	77–108	−0.98	±0.10	5.0	3.7	6.7	1.3
8.0	650	31–46	−0.95	±0.05	3.4	2.9	3.9	1.4
10.0	650	31–46	−1.01	±0.01	3.7	3.4	3.9	0.8

[a] α is the slope of a linear least-squares regression of $\log(100\sigma^2)$ vs $\log(H)$.
[b] $\hat{D}$ is from the intercept of the same linear regression, i.e. the intercept of $\log(100\sigma^2)$ vs $\log(H)$ is $2 + \log(\hat{D})$.

Table 5. Dimensionless dispersion coefficients least-squares regression results: $\sigma^2 = \hat{D}/H + \sigma_0^2$

ϕ (%)	$2a$ (μm)	$\hat{D}$ Mean	$\hat{D}$ 90% Confidence interval	$100\sigma_0^2$	R^{2a}	CV (%)
2.5	650	2.1	± 0.8	0.01	0.993	1.2
5.0	470	6.0	± 1.5	-0.09	0.991	2.0
	650	5.1	± 2.5	0.19	0.983	1.7
8.0	650	4.0	± 1.0	0.21	0.990	1.9
10.0	650	3.5	± 0.6	0.08	0.999	0.9

[a] R^2 = correlation coefficient (Myers 1986).

of H_∞ in our experiments is even less clear since we measured arrival times and not instantaneous speeds nor positions at fixed times. Therefore, for our purposes, H_∞ has been selected as the distance beyond which the measured variance shows consistent power law dependence upon H. This point was determined by examination of plots such as the one shown in figure 5a. Two statements can be made regarding H_∞: first, H_∞ is always greater than the 1 cm interval distance, despite serial correlations having shown little correlation between 1 cm interval speeds; second, the values are small enough to insure that a settling distance of 10–12.5 cm was sufficient to reach asymptotic behavior and provide adequate data to determine $\hat{D}$.

Dimensionless dispersion coefficients can be found from the log–log plots of σ^2 vs H, as shown in table 4, but once the random walk hypothesis has been verified more rigorous bounds for $\hat{D}$ can be found by taking $\hat{D}$ to be the slope of σ^2 vs $1/H$ in the limit as $1/H \to 0$ ($H \to \infty$). Figure 5b presents an example of σ^2 vs $1/H$ and the resulting least-squares line for $\phi = 5.0\%$ and $2a = 470\,\mu$m [see Ham (1988) for a complete set of figures]. The values of $\hat{D}$ calculated in this manner are given in table 5. Several important features of the results in table 5 are described in the following paragraph.

First, the 90% confidence intervals contained in table 5 reflect the 90% confidence intervals for the variance used in the regressions. These confidence intervals are roughly an order of magnitude larger than those arising simply from regressions of the expected values. If the values for the confidence limits in table 4 had been calculated in a similar fashion, then they, too, would have been correspondingly more widespread. Second, $\hat{D}$ in table 5 differs slightly from $\hat{D}$ calculated in table 4, since best-fit lines of σ^2 vs 1/H from our data do not pass exactly through to origin. The intercepts are, however, quite small and are simply reflections of experimental errors and of the confidence intervals on the variances. Finally, the dimensionless dispersion coefficients at 5.0% for the two different particle sizes each lie within the 90% confidence limits of the other. This indicates that the proposed scaling is not inconsistent with experimental results and provides evidence behavior is not an experimental artifact, e.g. a result of a bias in the initial mixing process.

Figure 6 shows the dimensionless dispersion coefficient to have a dependence upon concentration which is weak, but significant between $\phi = 2.5$ and 5%. The coefficient increases from 2 at $\phi = 25\%$ to 5–6 at 5%, then levels off or slightly decreases at higher concentrations. One possible explanation for the increase at low concentrations is an increase in the probability of multiparticle interactions as the concentration of particles increases. For example, at higher concentrations, an interacting pair of particles is more likely to interact with a third particle. These multibody interactions, as described in section 1, are an essential part of the mechanism leading to the random walk of a sedimenting particle. The leveling off or decrease at higher concentrations may be due to a restriction of particle movement as the interparticle distances become shorter, i.e. changes in the relative positions of particles are limited by the close proximity of nearest neighbors.

Figure 6 also contains a comparison of our results with the range of dimensionless dispersion coefficients reported by Davis & Hassen (1988). The comparison must be made with the understanding that Davis & Hassen inferred their coefficients from the initial spreading rate of an interface at the top of a sedimenting suspension, with the result that their determination was made with certain assumptions about polydispersity and hindered settling effects. Furthermore, their measurements were made in the presence of a gradient in volume concentration, and so quantitive agreement between the two sets of results cannot be expected since tracer and gradient diffusion

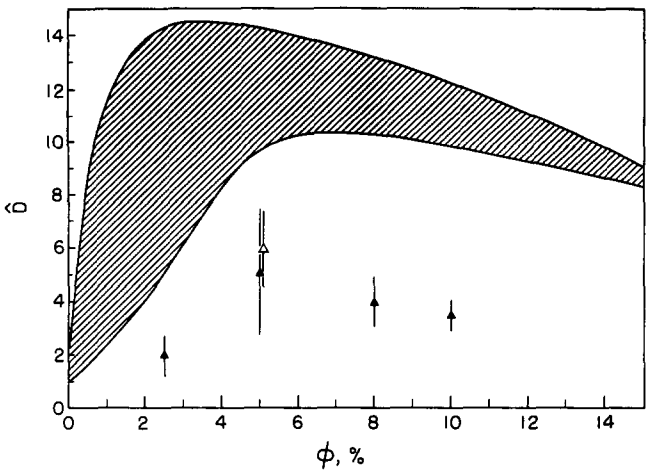

Figure 6. Experimental values of dimensionless dispersion coefficients: ▲, $2a = 650\ \mu$m; △, $2a = 470\ \mu$m; ▨, Davis & Hassen (1987). Error bars on the experimental values represent 90% confidence intervals.

are not, in general, equivalent, and their measurements represent an average over a concentration range. The two sets of coefficients are, however, of the same magnitude, with ours being somewhat lower than those of Davis & Hassen. More importantly, both experiments show coefficients which increase with concentration at low concentration and which plateau or decrease at higher concentrations. Surprisingly, both experiments show the change in behavior near a suspension concentration of 5%.

5. CONCLUSIONS

The hindered settling speed of an individual sphere internal to a random suspension has been measured directly for volume concentrations from 2.5 to 10%, under conditions of creeping flow and in the absence of Brownian motion. Scaling the mean settling speed with the Stokes settling speed is consistent with experimental results, as indicated by the close agreement of $\langle V \rangle / V_0$ for two different particle sizes at the same concentration. The resulting hindered settling function has an $O(\phi)$ coefficient below that determined for a "well-stirred" suspension. The discrepancy between our experiments and theoretical predictions is a strong indication of structure development even in suspensions which sediment from a random, thoroughly-mixed initial state.

The fluctuations in settling speed over relatively short settling distances have been found to be surprisingly large and the long-time (large settling distance) behavior of the variance in sedimentation speed has been shown to be that characteristic of a random walk, or Fickian diffusion process. Scaling the resulting dispersion coefficients with the product of hindered settling speed and particle radius is consistent with our data as indicated by the close agreement between the dimensionless coefficients for the two different particle sizes. The scaling agreement combined with the robust statistics produced by multiple, independent realizations are evidence that this dispersion phenomenon is a purely hydrodynamic effect, not an experimental artifact. The extremely low Reynolds numbers, the short time required for the phenomenon to appear, and, again, the close agreement between the coefficients for the two particle sizes, reduces the probability of this being an inertial effect. The large Brownian Péclet number, and the correspondingly large ratio of hydrodynamic dispersion to Brownian diffusion, eliminates the possibility of this being a Brownian motion effect. The observed dispersion is therefore concluded to be the results of viscous hydrodynamic interactions between suspended particles.

The dispersion coefficients found in our experiments are somewhat lower than those inferred by Davis & Hassen (1988). Quantitative agreement is not to be expected, owing to the difference between tracer and gradient diffusion. The agreement is, however, sufficient to provide additional confidence to the conclusion that hydrodynamic dispersion is an observable phenomenon.

Acknowledgements—This work was supported by the National Science Foundation Particulate and Multiphase Processing Section, under Grant No. NSF-17523. The authors wish to acknowledge the suggestions and stimulus for this work provided through previous discussions with Professor George Batchelor. Such discussions were made possible through a NATO Travel Grant. We also want to thank J. Kern Sears and Monsanto for assistance in identifying Santicizer 278 as the ideal fluid for these experiments and for donating a generous quantity of the fluid. Finally, special recognition and thanks must be given to Scott Thomas for his valiant assistance in performing many of these quite tedious experiments.

REFERENCES

BATCHELOR, G. K. 1972 Sedimentation in a dilute suspension of spheres. *J. Fluid Mech.* **52,** 245–268.

BATCHELOR, G. K. 1982 Sedimentation in a dilute polydisperse system of interacting spheres. Part 1. General theory. *J. Fluid Mech.* **119,** 379–408.

BATCHELOR, G. K. & WEN, C.-S. 1982 Sedimentation in a dilute polydisperse system of interacting spheres. Part 2. Numerical results. *J. Fluid Mech.* **124,** 495–528.

CAFLISCH, R. E. & LUKE, J. H. C. 1985 Variance in the sedimentation speed of a suspension. *Phys. Fluids* **28,** 759–760.

DAVIS, R. H. & BIRDSELL, K. H. 1988 Hindered settling of semidilute monodisperse and polydisperse suspensions. *AIChE Jl* **34,** 123–129.

DAVIS, R. H. & HASSEN, M. A. 1988 Spreading of the interface at the top of a slightly polydisperse sedimenting suspension. *J. Fluid Mech.* In press.

DURLOFSKY, L., BRADY, J. F. & BOSSIS, G. 1987 Dynamic simulation of hydrodynamically interacting particles. *J. Fluid Mech.* **180,** 21–49.

ECKSTEIN, E. C., BAILEY, D. G. & SHAPIRO, A. H. 1977 Self-diffusion of particles in shear flow of a suspension. *J. Fluid Mech.* **79,** 191–208.

HAM, J. M. 1988 Ph.D. Thesis, Stanford Univ., Stanford, Calif.

HINCH, E. J. 1977 An average-equation approach to particle interactions in a fluid suspension. *J. Fluid Mech.* **83,** 695–720.

LEIGHTON, D. & ACRIVOS, A. 1987 Measurement of shear-induced self-diffusion in concentrated suspensions of spheres. *J. Fluid Mech.* **177,** 109–131.

MEYER, P. L. 1970 *Introductory Probability and Statistics*, 2nd edn. Addison-Wesley, Reading, Mass.

MYERS, R. H. 1986 *Classical and Modern Regression with Applications.* Duxbury Press, Boston, Mass.

RICHARDSON, J. F. & ZAKI, W. N. 1954 Sedimentation and fluidization: Part I. *Trans. Instn chem. Engrs* **32,** 35–53.

SAFFMAN, P. G. 1973 On the setting speed of free and fixed suspension. *Stud. appl. Math.* **LII,** 115.

STRONG, J. 1938 *Procedures in Experimental Physics.* Prentice-Hall, Englewood Cliffs, N.J.